Ultrasound in Med. & Biol., Vol. 40, No. 4, pp. 655–674, 2014

0301-5629/$ - see front matter

http://dx.doi.org/10.1016/j.ultrasmedbio.2013.11.001

● *Review for the Festschrift in honor of Robert C. Waag*

PHYSICAL MODELS OF TISSUE IN SHEAR FIELDS[1]

EDWIN L. CARSTENSEN and KEVIN J. PARKER
Department of Electrical and Computer Engineering and Department of Biomedical Engineering, University of Rochester, Rochester, New York, USA

(*Received* 30 *April* 2013; *revised* 1 *October* 2013; *in final form* 4 *November* 2013)

Abstract—This review considers three general classes of physical as opposed to phenomenological models of the shear elasticity of tissues. The *first* is simple viscoelasticity. This model has a special role in elastography because it is the language in which experimental and clinical data are communicated. The *second* class of models involves acoustic relaxation, in which the medium contains inner time-dependent systems that are driven through the external bulk medium. Hysteresis, the phenomenon characterizing the *third* class of models, involves losses that are related to strain rather than time rate of change of strain. In contrast to the vast efforts given to tissue characterization through their bulk moduli over the last half-century, similar research using low-frequency shear data is in its infancy. Rather than a neat summary of existing facts, this essay is a framework for hypothesis generation—guessing what physical mechanisms give tissues their shear properties. (E-mail: ecarsten@rochester.rr.com) © **2014 World Federation for Ultrasound in Medicine & Biology.**

Key Words: **Shear elasticity, Viscoelasticity, Shear relaxation, Hysteresis, Shear waves, Shear models.**

INTRODUCTION

After it became apparent more than a half century ago that ultrasound had a firm place in both medical diagnosis and therapy, a parallel investigative effort to understand the mechanisms responsible for the acoustic properties of tissues was undertaken. For the irrotational, largely compressional waves employed in most applications of diagnostic ultrasound, the bulk moduli and densities of soft tissues, on which imaging depends, differ from one to another by only a few percent (Goss et al. 1978). Acoustic absorptions in tissues even at megahertz frequencies are modest. Modern diagnostic ultrasound systems have adapted to these properties and produce high-resolution images at large depths of penetration.

The absorptions associated with the propagation of irrotational waves are consistent with models involving acoustic relaxation at the macromolecular level (Duck et al. 1998). Even solutions of a single molecular species such as hemoglobin appear to involve many different relaxation processes with a broad distribution of relaxation times (*e.g.,* Carstensen and Schwan 1959b). Other, largely phenomenological models for tissue properties have been proposed, and research on this subject continues today. However, models based on chemical or structural relaxation at the macromolecular level are consistent with available observations. In fact, because it is possible to invoke arbitrary distributions of relaxation processes to match nearly any observed frequency dependence for the absorption, relaxation models are difficult to disprove. Structure makes a modest contribution to absorption (Carstensen and Schwan 1959a; Pauly and Schwan 1971). Professor Waag has contributed fundamentally to an understanding of ultrasound propagation through macroscopically inhomogeneous tissues (*e.g.,* Mast et al. 1999; Nachman et al. 1990; Salahura et al. 2010).

For years, the use of shear waves in diagnostic medicine languished because of their large absorption coefficients. That changed with the invention of elastography, which uses shear strains and shear waves at extremely low frequencies, where propagation even in soft tissues can extend to useful distances (Parker et al. 2011). Progress in the development of elastography as a diagnostic tool has accelerated over the last two decades, but we have yet to undertake an in-depth study of the mechanisms responsible for the shear properties of tissues.

Address correspondence to: Edwin L. Carstensen, 103 Eastland Avenue, Rochester, NY 14618-1027, USA. E-mail: ecarsten@rochester.rr.com

[1] This article is dedicated to our friend and colleague, Robert C. Waag.

There are several reasons to believe that such studies will be even more valuable than they have been for compressional wave propagation. First, the shear moduli of soft tissues are five or six orders of magnitude smaller than their bulk moduli (Gao et al. 1996; Sarvazyan et al. 1995). Furthermore, the effective shear viscosities of soft tissues reported at audible frequencies (Boursier et al. 2009; Deffieux et al. 2007; Zhang et al. 2007) are several orders of magnitude greater than they are at megahertz frequencies (Frizzell et al. 1976). Those properties alone suggest that we can expect qualitatively different information about tissues from elastography than we have learned from compressional wave probes of soft tissues. Most important, in contrast to the case for compressional waves, it turns out that the shear moduli of diseased tissues, in many cases, are an order of magnitude or more greater than they are for normal soft tissue, making the value of the shear modulus itself a useful diagnostic datum. Today, we know from many independent studies that there is a rough correlation between shear modulus of liver and its degree of fibrosis as assessed qualitatively through biopsy (Carstensen et al. 2008; Sandrin et al. 2003). Because shear modulus can be measured non-invasively and quantitatively, there is reason to hope that it can eventually provide the diagnostic baseline to which other diagnostic data are referenced in the management of liver disease.

Empirical or phenomenological descriptions of observed data are useful even though they tell us little or nothing about the underlying physical processes. Our purpose in this review, however, is to start first with guesses about what it is in the structure and behavior of tissue that controls its shear properties and, then, to formulate these guesses into models that are sufficiently specific and quantitative that they can be tested experimentally. Of course, all knowledge is faith—guesses or models of the truth that to the best of our experience, directly or indirectly, are consistent with observations of the real world. This essay is more a framework of guesses than a review of tested models. In the long run, however, there is great hope that physically based models will elucidate the diagnostically relevant information that elastography promises.

Our knowledge for shear elasticity as it applies to elastography is at approximately the stage of development that the theory for compressional wave propagation was a half-century ago. And, the opportunities for study are almost completely open to us. There is hope, however, that progress can be more rapid in shear wave studies, in part because of the guidance we may find in the similar effort that has been made over the years in the study of irrotational wave propagation.

The terms *stiffness* and *compliance* are generic descriptors of the difficulty or ease of distorting objects or the materials from which they are made. At one extreme, we might have the stiffness of a coiled spring that could be quantified as a simple 1-D scalar relationship between force applied and its change in length. At the other extreme, to describe the material properties of the steel from which it is made, we need fourth-order stiffness tensors to relate the second-order stresses applied to the material to the second-order strains. Such formulations permit us to deal with materials that are anisotropic. Certain tissues such as muscle are in fact strongly anisotropic. Although this discussion is limited to purely isotropic materials, the need to deal with more complex media in the long run should not be ignored.

The stiffness of an isotropic medium can be characterized by two moduli: the bulk modulus, κ, the ratio of the mean normal stresses on an element of the material to its volume change, and the shear modulus, μ, the ratio of shear stress to shear strain, which characterizes the change in shape of the element. It is the shear modulus of tissue that has been found to change profoundly in certain diseased states; it is the shear modulus that is the focus of elastography, and physical models of the shear modulus are the subject of this discussion. As we illustrate, when stress and strain are purely shear, it is possible to reduce the general tensor equations to simple scalar statements, thus greatly simplifying our presentation. It is possible to design laboratory experiments that involve only shear. All medical applications of elastography involve both shear and bulk strains. However, shear strains in these applications are orders of magnitude greater than bulk strains.

Although no model is ever the full truth, all we ask is that it be "true enough" to be useful. Of the general classes of models for soft tissues (Delingette 1998; Fung 1981; Humphrey 2003), we consider three. The *first* is simple viscoelasticity. It assumes that each element of tissue has shear stiffness and coincident shear viscosity—each quantity independent of time and frequency. It says that shear stress is proportional not only to the strain itself, but also to the time rate of change of strain. Despite its simplicity, this model has a special role in elastography because it is the language in which experimental and clinical data are communicated. In fact, the first generation of clinical elastography systems makes no effort to describe the frequency or rate dependence of shear tissue properties.

As noted earlier, the shear viscosity of soft tissues, as seen through the simple viscoelastic model, is strongly frequency dependent. For the broader picture, therefore, more complex models are required. This *second* class of models involves acoustic relaxation, in which the medium contains inner time-dependent systems that are driven through the external bulk medium. The stress response with relaxation is dependent on both strain

and time rate of change of strain as in the simple viscoelastic model. The response is just somewhat more complicated. Most of the observed shear properties of tissues can be described with relaxation models.

The *third* class of models is somewhat more speculative. There is some evidence that when tissues are strained they do not return spontaneously to their native state as would be expected for a viscoelastic or relaxation medium, for example, pitting edema. For behaviors like this, the absorptions are related to strain rather than time rate of change of strain, the processes are almost always non-linear, the models may not be causal and the wave speed may be dispersionless, that is, independent of frequency. This process is called *hysteresis*.

It will be readily apparent that this is not a tutorial, a neat summary of existing facts, but rather an invitation to the reader to collaborate in the development of more accurate and elaborate conceptual physical models of the shear properties of tissues and the potential relationships of these models to diagnostic medicine.

Our primary motivation for this review has been to develop an intuitive picture of tissues and their shear properties. It is our hope that by erring on the side of qualitative description, we can prevent the trees from obscuring the forest. In that spirit, we provide next an overview of our review.

Part I is just Newton's second law of motion (force = mass $\times$ acceleration) applied to a linear elastic continuum. When we apply the law to a continuous medium instead of a simple object, our problem is complicated by the need to decide what the "object" is to which we apply the force. As a result, our modified Newton's law relates *elastic force density*, or force per unit volume, to the *inertial force density* involving the acceleration of mass per unit volume.

We write the force density as the divergence of the stress in the medium; the stress is the force per unit area, and its divergence is the space rate of change of the stress and, hence, the net force per unit volume. It takes a package of three scalar numbers to specify a force (a vector or first-order tensor) and nine scalars to specify a stress state or stress tensor (a second-order tensor). The stress tensor is symmetric, so at most six of its scalar elements are independent. The science of acoustics, in general, deals with fluids. In that case, the force per unit area in the medium is the same in all directions and always normal to any surface. This simplification means that the stress can be characterized by a single, time- and space-dependent, scalar number. In acoustics, that scalar is called the pressure. Of course, pressure is a stress (a force per unit area and a second-order tensor), but it can be treated as a scalar in basic acoustics. The force density of the pressure, when treated as a scalar, is its gradient. It happens that the gradient of the pressure treated as a scalar is equal to its divergence when treated as a second-order tensor. It is quite remarkable that almost the entire theory behind diagnostic ultrasound starts with the acoustic assumption, that is, tissue is a fluid.

Of course, shear waves cannot propagate in fluids. We will see that elastography is possible because soft tissues fall in a narrow window of shear moduli and shear viscosities where shear stiffnesses are large enough to support wave propagation and viscous losses are small enough that they can travel useful distances.

Whether our focus is on diagnosis, safety or therapy, we are interested in what happens to tissue when it is subjected to mechanical stress. We quantify the tissue response by its strain. Despite the central role that strain plays, conventional diagnostic ultrasound can be practiced without giving it much thought. That, in part, is because compressional strain is so small—of the order of 0.001 at the highest pressure levels permitted under Food and Drug Administration guidelines. Those transient pressures are nearly 2 MPa. That is roughly the pressure one would experience under water at about 200 m. In fact, the small strains may account for the fact that huge transient pressures can be used in conventional diagnostic procedures with no apparent effect on the tissues. The shear strains we employ in elastography are another story.

Strain comes in two flavors: bulk strain, which measures change in volume, and shear strain, which measures change in shape of the medium. Both occur in conventional diagnostic ultrasound. In that application, however, they are of the same order of magnitude and very small. In elastography, shear strains are of the order of a few percent despite the fact that the shear stresses are of the order of a kilopascal—five or six orders of magnitude smaller than the stresses used in conventional diagnostic ultrasound. Depending on the point of view of the observer, shear strain may look like changing a cross section of the medium from a square to a parallelogram or from a square to a rectangle. For pure shear strain these shape changes take place without change in the volume occupied by the element.

In the same way that we use Hooke's law to relate the stretching of a spring to the force applied, we can relate stress to strain using a generalized Hooke's law. Arbitrary, realistic applications relating stress to strain can become rather complicated. However, it is possible to choose examples that illustrate the basic physical processes with minimal mathematical complications. For a linear, elastic, isotropic material at the most basic level, the ratio of dilatational stresses to bulk strain is called the *bulk modulus*, and the ratio of shear stress to shear strain is given by the *shear modulus*.

If one element of a continuous medium is strained, it affects its neighboring elements and the strain

propagates throughout the medium. The rate of propagation is determined by the elastic moduli of the medium. One of the most attractive methods for measuring these moduli involves measurements of the dynamics of that propagation. Part I simply elaborates on this propagation. Discussion of the three classes of physical models of the shear properties of tissues is taken up in Part II.

PART I: SHEAR STRAIN IN WAVE PROPAGATION

The wave

For our purposes, it can be assumed that Newton's second law is valid for any physical object; that is, its acceleration is equal to the force acting on it. In a continuum, this can be stated in terms of forces per unit volume, or *force densities*,

$$\nabla \cdot \overrightarrow{\overrightarrow{T}} + \overrightarrow{F}_b = \rho \frac{D^2 \overrightarrow{\xi}}{Dt^2} \tag{1}$$

where ρ is density, t is time and $\overrightarrow{\xi}$ is particle displacement. (For linear systems where the amplitude of oscillation is small, the total time derivative in eqn [1] can be replaced by the partial time derivative.) Force densities may be viewed as arising from either (i) an imbalance in surface forces (first term), (ii) as "generated" internally, for example, gravity or radiation force associated with the absorption of ultrasound (second term) or (iii) inertial forces (third term). The components of the stress tensor $\overrightarrow{\overrightarrow{T}}$ consist of the components of the vector forces per unit area on each of three orthogonal surfaces. Specifying the stress requires a second-order tensor composed of nine scalars. However, stress, by convention, includes only forces that change volume or shape of the medium. That makes the stress tensor symmetric, and at most six of its scalar elements are independent. (See eqn [17] and associated Fig. 4.)

Stress and strain are related through a generalized form of Hooke's law. If we rewrite the stress in eqn (1) in terms of the strain, the relation involves just one vector-dependent variable, the particle displacement, $\overrightarrow{\xi}$.

$$\overrightarrow{\overrightarrow{T}} = \overrightarrow{\overrightarrow{c}} \cdot \overrightarrow{\overrightarrow{S}} \tag{2}$$

where $S_{ij} = \frac{1}{2}(\partial \xi_i / \partial x_j + \partial \xi_j / \partial x_i)$ and $\overrightarrow{\overrightarrow{c}}$ is the fourth-order stiffness tensor, which relates stress to strain, x_i and ξ_i being the spatial coordinate and element of the displacement vector, respectively. Written in this form, it looks like Hooke's law for a simple mechanical spring. That is essentially what it is. The compact notation helps us feel the basic physics. In this case, however, we can generate revealing, simple, special cases by looking under the hood.

The simplest medium we can choose that is relevant to the propagation of shear strains is an isotropic solid. In greater detail for that case, eqn (2) is

$$\begin{bmatrix} T_{11} & T_{22} & T_{33} & T_{12} & T_{13} & T_{23} \end{bmatrix} = \begin{bmatrix} \kappa+\frac{4}{3}\mu & \kappa-\frac{2}{3}\mu & \kappa-\frac{2}{3}\mu & 0 & 0 & 0 \\ \kappa-\frac{2}{3}\mu & \kappa+\frac{4}{3}\mu & \kappa-\frac{2}{3}\mu & 0 & 0 & 0 \\ \kappa-\frac{2}{3}\mu & \kappa-\frac{2}{3}\mu & \kappa+\frac{4}{3}\mu & 0 & 0 & 0 \\ 0 & 0 & 0 & 2\mu & 0 & 0 \\ 0 & 0 & 0 & 0 & 2\mu & 0 \\ 0 & 0 & 0 & 0 & 0 & 2\mu \end{bmatrix} \cdot \begin{bmatrix} S_{11} \\ S_{22} \\ S_{33} \\ S_{12} \\ S_{13} \\ S_{23} \end{bmatrix} \tag{3}$$

where T_{ij} are the elements of the symmetric stress tensor $\overrightarrow{\overrightarrow{T}}$. In this way, the bulk modulus κ of the medium and its shear modulus μ relate the stress tensor to the strain tensor.

Although certain tissues are significantly anisotropic, and at some level, all tissues are non-linear, dealing with these additional complexities would be more confusing than helpful in our discussion of basic tissue models. Therefore, we will assume throughout that tissue is isotropic and that its elastic properties are not changed by strains in the medium.

We can precisely determine the stiffness of a spring by applying a force to one end and measuring its change in length. In principle, we can measure the stiffness of tissue by applying a stress and measuring the strain. We need stress and strain fields, however, not single numbers—a somewhat greater challenge. Actually, the differences among tissues' shear moduli are so high that it is possible produce useful, semi-quantitative diagnostic images simply by showing strain

alone without a detailed knowledge of the stresses that produce them.

There is, however, a qualitatively different approach that is particularly attractive for precision measurement of tissue stiffness. Although both shear and compressional waves may be generated in tissue, the wave speeds differ so greatly that it is easy to observe the shear wave without interference of other acoustic activity in the medium. Furthermore, it turns out that the speed of travel of shear waves depends only on the slow shear modulus and density. Thus, as long as the shear wave speed can be determined, it is unnecessary to have any quantitative information about the magnitudes of the stresses or strains involved. It is even possible to create elastographic images of the tissues based on the speed of the shear wave as it propagates. This discussion will be confined wholly to studies of tissue properties through wave propagation.

Substituting eqn (3) into eqn (1) yields

$$\left(\kappa+\frac{4}{3}\mu\right)\nabla\nabla\cdot\vec{\xi}-\mu\nabla\times\nabla\times\vec{\xi}+\vec{F}_b=\rho\frac{\partial^2\vec{\xi}}{\partial t^2} \quad (4)$$

which Graff (1975:283–288) and other authors assure us is valid in all coordinate systems. In this form, eqn (4) separates the dilatation $\Delta V/V=\nabla\cdot\vec{\xi}=Tr\vec{\vec{S}}=S_{11}+S_{22}+S_{33}$ from the rotation $\vec{\Omega}=\nabla\times\vec{\xi}$. Because the divergence of the curl and the curl of the divergence of a vector are each zero, one can obtain equations for pure dilatational waves by taking the divergence of each side of eqn (4) and, for pure rotational waves, by taking the curl of both sides:

$$\left(\kappa+\frac{4}{3}\mu\right)\nabla^2\frac{\nabla V}{V}+\nabla\cdot\vec{F}_b=\rho\frac{\partial^2\frac{\Delta V}{V}}{\partial t^2} \quad (5)$$

and

$$-\mu\nabla\times\nabla\times\vec{\Omega}+\nabla\times\vec{F}_b=\rho\frac{\partial^2\vec{\Omega}}{\partial t^2} \quad (6)$$

and with the vector identity,

$$\nabla^2\vec{\Omega}=\nabla\nabla\cdot\vec{\Omega}-\nabla\times\nabla\times\vec{\Omega} \quad (7)$$

$$\mu\nabla^2\vec{\Omega}+\nabla\times\vec{F}_b=\rho\frac{\partial^2\vec{\Omega}}{\partial t^2} \quad (8)$$

The wave from eqn (5) tells us that dilatations and compressions move through media with a speed

$$c_d=\sqrt{\frac{\kappa+\frac{4}{3}\mu}{\rho}} \quad (9)$$

Similarly eqns (6) through (8) say that the slow wave speed of rotational (incompressible/shear) waves in elastic media is

$$c_s=\sqrt{\frac{\mu}{\rho}} \quad (10)$$

Because bulk moduli of tissues are many orders of magnitude greater than their shear moduli, dilatational wave speeds and wavelengths are much greater than those of incompressible, rotational waves at the same frequency. Although both waves are generated in elastography, when the excitation is a very short pulse (*e.g.,* transient and radiation force elastography), they quickly separate spatially and can be treated independently.

As shown in eqns (5) and (8), the precise characterization for the two qualitatively different modes of elastic wave propagation should probably be incompressible and irrotational. These negative terms are frequently approximated with the more intuitive terms "shear, transverse, or rotational" and "compressional or longitudinal," although we can have longitudinal shear waves and longitudinal, compressional waves that involve shear strain.

With one exception, the displacements, or waves, used in elastography are generated by surface forces (Parker et al. 2011). Surface forces currently used in elastography include (i) continuous sinusoidal excitation (sono-elastography [Lerner et al. 1988. 1990]); (ii) step functions (sometimes called "compression elastography" [Ophir et al. 1991]); and (iii) single cycle (sometimes referred to as "transient elastography" [Sandrin et al. 2003; Bercoff et al. 2004]). In the second case, time-dependent shear strains are computed directly from ultrasonically measured displacements of the media. From these time-dependent strains, it is possible in principle to determine the complex shear modulus of the medium (Amador et al. 2012). In the first and third cases, complex shear moduli of the media are inferred from characteristics of the shear waves generated by the surface forces. Images may be formed directly from displacements of the media or through measurements of shear wave speed in the tissues. In all realistic applications of elastography, both compressional/dilatational and shear strains waves are generated. In fact, the particle displacements associated with both strains are comparable. However, the shear strains are orders of magnitude greater than the compressional strains, and the shear wave speeds are far smaller than the compressional wave speeds. Of course, elastography is concerned with shear phenomena.

The exception noted above is radiation force elastography (Fatemi and Greenleaf 1998; Sarvazyan et al. 1998; Nightingale et al. 1999; Nightingale et al. 2001; Bercoff et al. 2004; McAleavey et al. 2009), in which

the externally applied source of shear waves comes from the absorption within the tissue of externally applied high-frequency ultrasound. We have carried the term $\vec{F}_b$ in eqn (1) to this point to show the way that they drive dilatational and rotational waves when they are present. These sources are irrelevant to our discussion of tissue models and will be dropped at this point.

In isotropic media, each element can be characterized by a coincident mass and two stiffnesses: one that controls the volume of the element and a second that controls its shape. Now assume that a piston exerts a sudden (∼step function), inwardly directed force normal to the surface of a semi-infinite medium. Elements of the medium adjacent to the surface accelerate forward, creating strains and corresponding stresses in the medium. The applied force is balanced first by the inertial forces of the accelerating mass and, subsequently, by the stiffness of the medium as it becomes strained. The divergence of the stresses becomes force densities that accelerate the elements next in line, which in turn repeat the process, initiating a wave of longitudinal displacements and strains traveling into the medium with a speed given by eqn (9).

In the longitudinal wave just described, elements of the medium change both their volumes and their shapes. In comparison, applying a force tangentially to the surface of same medium changes the shape of the elements of the medium without change in volume. Because of the relatively small shear stiffnesses involved, the amplitudes of displacements in tissues are much greater than they would have been for longitudinal waves of the same frequency and stress.

The characterization of the medium by coincident mass and stiffness suggests the possibility of a corresponding resonance frequency. In fact, if the tissue sample is confined between reflecting surfaces, the pulse that we generated above will be returned from the far interface. If we time our subsequent pulse to correspond with the second reflection from the near surface, we can build up the amplitude of the displacement just as we would to a swing in the playground or the air in an organ pipe (standing waves). The resonance frequency is determined by the dimensions of the container, however. It is not an intrinsic property of the tissue.

Equations (5) and (8) are informative, but in the general case, we need a wave that includes both bulk and shear strains and, furthermore, explicitly involves the particle displacement, which is the parameter that is directly observed in elastography. So, we return to eqn (4), keeping in mind that in tissue, bulk moduli are many orders of magnitude greater than shear moduli.

In an elastic medium $(\mu \neq 0)$, the normal stresses need not be equal, but by using eqn (3) we can define without approximation

$$\tau = \frac{T_{11}+T_{22}+T_{33}}{3} = \kappa \nabla \cdot \vec{\xi} = \kappa \frac{\Delta V}{V} = \kappa \mathrm{Tr}\,\vec{\vec{S}} \qquad (11)$$

where $\mathrm{Tr}\,\vec{\vec{S}}$ is the sum of the diagonal elements, the trace, of the strain tensor, and the scalar τ then is the mean of the normal stress components. It is the negative of the scalar pressure as used in acoustics. In soft tissues, where shear and bulk moduli are of the order of 1 kPa and 1 GPa, respectively,

$$\left(\kappa + \frac{4}{3}\mu\right) \nabla \nabla \cdot \vec{\xi} \sim \nabla \tau \qquad (12)$$

to an accuracy of one part in a million (eqn [3]). In other words, τ and $-p$ (pressure) differ only conceptually, and the first term of eqn (4) can now be seen as the gradient of the scalar, mean, bulk stress. It is entirely dilatational and travels with the corresponding wave speed (eqn [9]).

Oestreicher (1951), among the first contributors to the bioacoustics of tissues, identified this "mean" normal stress with the negative pressure in acoustics and used it as a convenience in his treatment of the field of an oscillating sphere in a viscoelastic medium. This quantity should not be confused with "average" normal stress, which, in mechanics, is frequently used to identify the average of the forces over an arbitrary finite surface area.

The second term in eqn (4) can be written with roughly the same accuracy as the vector Laplacian of the displacement, yielding with minimal approximation

$$\nabla \tau + \mu \nabla^2 \vec{\xi} = \rho \frac{\partial^2 \vec{\xi}}{\partial t^2} \qquad (13)$$

Each of the terms in this general wave equation is a force density. Actually, eqn (13) is a set of six scalar equations, each of which must be satisfied independently—an equation for each of the real and the imaginary components of each of the orthogonal components of the 3-D vector $\vec{\xi}$.

Thus written, the wave equation is remarkably informative. It is completely general in the sense that it includes the contributions and interactions of both shear and compressional waves to the particle displacement. The first term is the force density associated with dilatation and has a propagation speed of c_d. The second is associated with shear and propagates at a speed of c_s. From the point of view of elastography, because c_d is two to three orders of magnitude greater than c_s, the dilatational wave effectively illuminates an entire organ simultaneously. It is a bit like walking through a room (slow, shear wave) that is lit by a flashing sign from across the street (fast, dilatational wave). The light may be brighter near the window, but the whole room goes light and dark at the same time.

Relative importance of shear and compression

In any biomedical application it is natural to ask when, or under what conditions, we can ignore any of the terms in eqn (13). More generally, we wish to determine the relative importance of shear, compression and acceleration (inertial) terms. The classic example in Graff (1975:356) shows an oscillating indentor on a semi-infinite half-space and the resulting partition into shear, compressional and Rayleigh (surface) waves. However, the relative contributions are highly dependent on particular values of material parameters, geometry and frequency.

As an interesting example, when you palpate your liver, the normal stress you apply with your fingers is transmitted throughout the organ in times on the order of 100 μs. The dilatational stresses are not spatially uniform, of course. They decrease with distance from your fingers. The dilatational stress on its own causes almost no change in the tissue because of its huge bulk modulus. For almost a millisecond, the tissue is essentially rigid, and then, in response to the shear stresses that your fingers generate at the surface of the skin, elements of the tissue begin to change shape and relatively large displacements occur. It is important to emphasize that those shear stresses are both normal and transverse; that is, they come from diagonal and off-diagonal elements in the stress tensor.

Because the terms on the left are second-order spatial rates of change, comparison of the magnitudes of those terms depends strongly on the geometry of the application. Rather than try to generalize, we use a single example that is relevant to all forms of elastography. Oestreicher's (1951) solution for the displacement field of a translating sphere is perhaps the best analytical model for this purpose. His solution in spherical coordinates (r, θ, ϕ) chosen with the axis of oscillation at $\theta = 0$ is

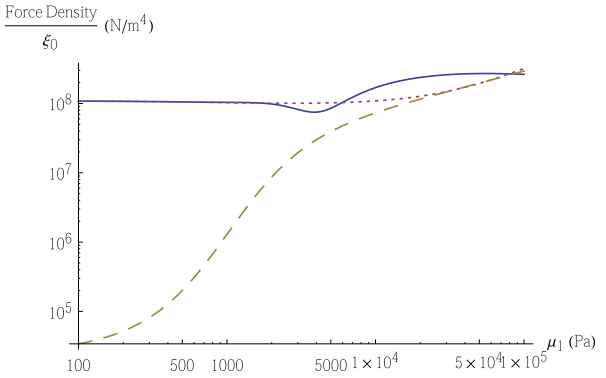

Fig. 1. Absolute magnitudes of the normalized radial components of the force densities in eqn (13) as a function of the real shear modulus of the medium—the compressional term (c_d = 1500 m/s, *dotted line*), the shear term (*dashed line*) and their sum (*solid line*). (Note that signs of the compressional and shear terms are opposite, and hence the solid curve is the difference of the plotted absolute values.) Radius of sphere = 1 cm, absorption coefficient of the shear component = 212 m^{-1}, its phase velocity = 2.4 m/s, density of medium = 1000 kg/m^3, point of observation r = 2 cm, $\theta = \pi/4$, frequency = 1000 rad/s. All values normalized to the source displacement. All computations *via* Mathematica (Wolfram, Champaign, IL, USA).

$$\xi_r = \xi_0 \cos\theta \frac{a^3}{r^3}\left\{\frac{e^{-jk(r-a)}\left(3+3jha-(ha)^2\right)\left(-2-j2kr+(kr)^2\right)}{\left(2+2jka-(ka)^2\right)(ha)^2+(ka)^2(1+jha)}+\frac{e^{-jh(r-a)}2\left(3+3jka-(ka)^2\right)(1+jhr)}{\left(2+2jka-(ka)^2\right)(ha)^2+(ka)^2(1+jha)}\right\}$$
$$\xi_\theta = -\xi_0 \sin\theta \frac{a^3}{r^3}\left\{\frac{e^{-j(kr-a)}\left(3+3jha-(ha)^2\right)(1+jkr)}{\left(2+2jka-(ka)^2\right)(ha)^2+(ka)^2(1+jha)}-\frac{e^{-j(hr-a)}\left(3+3jka-(ka)^2\right)\left(1+jhr-(hr)^2\right)}{\left(2+2jka-(ka)^2\right)(ha)^2+(ka)^2(1+jha)}\right\} \quad (14)$$

where a is the radius of the sphere, $k = \omega/c_d$ is the propagation constant for dilatational waves, $h = \omega/c_s$ is the propagation constant for shear waves and ω is the angular frequency. The equations for ξ_r and ξ_θ each have two groups of terms within the brackets. The first group propagates with a speed $c_d = \omega/k$, and the second group propagates as $c_s = \omega/h$. These are the compressional and shear components, respectively. As we will see in the next section, for steady-state conditions involving a single frequency, we can include absorption simply by letting the propagation constants be complex numbers, for example, $h = \beta - j\alpha$. At frequencies used in elastography, the absorption coefficients of compressional waves are so small that we have always assumed the k is real.

Figure 1 gives the absolute magnitude of the radial component of the two terms on the left side of eqn (13) and their sum as the propagating medium morphs from liquid to a solid. The parameters chosen for the illustration are more or less representative of those found in elastographic applications. Absorption coefficients associated with the dilatational component of the wave are assumed to be negligible. The value of the absorption coefficient for the shear component of the wave corresponds to that of a viscoelastic medium (see description in Part II) having a shear modulus of 1 kPa and a viscosity of 1 Pa s. The plateau at small values of the real part of the shear

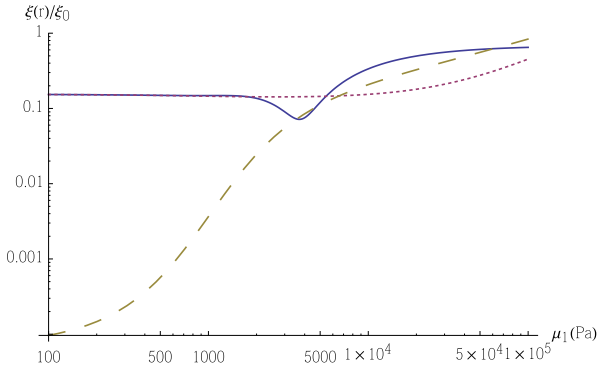

Fig. 2. Absolute value of the radial component of the displacement. All parameters are the same as in Figure 1, except $\theta = 0$.

modulus μ_1 is determined by that viscosity. The shear moduli of most soft tissues fall in the range 1–10 kPa. Serendipitously, that is the region in which the general wave equation becomes strongly dependent on the shear. Below 1 kPa, the medium looks much like a viscous fluid. It is apparent that the force densities for the fast and slow components of the wave are both important in the region of interest to elastography.

Of course, elastography directly detects the displacement or its time derivative. When the excitation source is at the surface of the body, the radial component of the displacement is a fair approximation of the measured quantity. Radiation force elastography tends to view the tangential displacements. Figures 2 and 3 illustrate these two displacements for the conditions chosen in Figure 1. Again, we find the propagating medium behaving like a viscous liquid for shear moduli below 1 kPa. That is to say, for shear moduli less than 1 kPa, the complex shear modulus at $\omega = 1000$ radians/s is dominated by viscosity rather than real stiffness. In the region 1–10 kPa, the two waves interfere constructively and destructively. Above 10 kPa, phase differences between the two components approach π, leading to a new plateau in the value of the displacement. Throughout, we deal

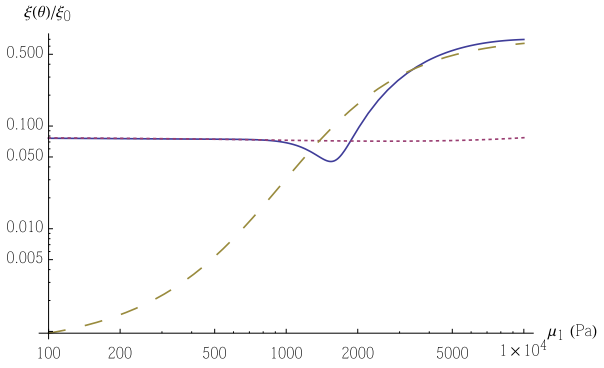

Fig. 3. Absolute value of the tangential component of the displacement. All parameters are the same as in Figure 1, except $\theta = \pi/2$.

specifically with single-frequency, continuous waves. It is worth mentioning, however, that with transient or radiation force elastography, the dashed and dotted components in Figures 2 and 3 would separate spatially a short distance from the sphere and there would be no solid curve. This not only has implications conceptually, but may be important practically in the design of equipment for use in elastography.

Investigation of the field of the sphere reveals a number of interesting details. For example, the strain along the axis of oscillation is almost entirely shear despite the fact that the particle displacement is entirely radial and longitudinal. Compressional strain along the axis is many orders of magnitude smaller than shear strain. Particle displacement at $\theta = \pi/2$, is tangential and transverse, compressional strain is zero and shear strain is entirely transverse.

The discussion up to this point provides some suggestions of the phenomena that elastographers deal with in measuring the shear modulus of tissues in diagnostically useful terms. However, we have given little detail about the characteristics of shear strain itself.

Shear strain

With the proper choice of coordinate system, we can resolve the particle displacement vector $\vec{\xi}$ that characterizes an arbitrary mechanical wave into two components: one in the direction of propagation, the longitudinal component, and one transverse to the direction of propagation. The longitudinal component is potentially a bit involved, so for the purposes of the discussion of shear strain let us begin with a wave that is entirely transverse.

We generate an infinite plane, transverse wave in the x_1 direction in tissue by stressing the x_1 surface, whose normal is parallel to the x_1 axis, tangentially in the x_2 direction at an angular frequency of ω. The only displacements in the medium will be in the x_2 direction, and they will be a function only of the spatial variable x_1. These assumptions make $\tau = 0$ (eqns [12] and [13]), and furthermore, of the six independent equations contained in the general wave equation (eqn [13]), we are left only with the two concerned with force densities in the x_2 direction.

$$\mu \frac{\partial^2 \xi_2}{\partial x_1^2} \vec{e}_2 = \rho \frac{\partial^2 \xi_2}{\partial t^2} \vec{e}_2 \tag{15}$$

where $\vec{e}_2$ is the unit vector in the x_2 direction. The initial assumptions tell us that the solution to the equation will have the form

$$\vec{\xi}_2(x_1, t) = \xi_0 e^{j(\omega t - h x_1)} \vec{e}_2 \tag{16}$$

If $h = \omega/\sqrt{(\mu/\rho)} = \omega/c_s$. The amplitude of the displacement, ξ_0, is directly proportional to the applied surface stress.

Now, let us retrace the physical processes leading up to this form of the wave equation (eqn [15]). As the wave progresses, we can describe the change of the medium at a microscopic level by its displacement gradient (the outer product of the vector del operator with $\vec{\xi}_2$— the left-hand side of eqn [16]). We can write the displacement tensor as the sum of its symmetric and anti-symmetric components, the strain and the rotation, respectively. The trace of the strain tensor is zero, telling us that there is no volume change in an element of the medium. As shown pictorially in Figure 4, the off-diagonal elements describe the change in shape of the element and, indirectly, the elastic stresses that would return it to its original shape.

$$\frac{\partial \xi_2}{\partial x_1}\begin{bmatrix}0&1&0\\0&0&0\\0&0&0\end{bmatrix}=\frac{1}{2}\frac{\partial \xi_2}{\partial x_1}\begin{bmatrix}0&1&0\\1&0&0\\0&0&0\end{bmatrix}+\frac{1}{2}\frac{\partial \xi_2}{\partial x_1}\begin{bmatrix}0&1&0\\-1&0&0\\0&0&0\end{bmatrix} \tag{17}$$

The shear strain itself does not involve a net movement of the medium. It simply describes the change of shape of the elements of the medium. Rotation, in contrast, is the embodiment of the inertial term of the transverse wave equation in the same sense that translation is for irrotational waves. The anti-symmetric rotation tensor is the equivalent of $\nabla\times\vec{\xi}$ as the rotation appeared in the purely vector language used in eqn (4). These are just two mathematical conventions for describing the rigid rotation of the medium. Elastic restoring stresses are related only to the shear strain. Employing eqn (3) gives us that restoring stress for our example.

$$\vec{\vec{T}}=\mu\frac{\partial \xi_2}{\partial x_1}\begin{bmatrix}0&1&0\\1&0&0\\0&0&0\end{bmatrix} \tag{18}$$

The divergence of the stress gives us the elastic force density that drives the rotation and creates the strain of the element of the medium.

$$\nabla\cdot\vec{\vec{T}}=\mu\begin{bmatrix}\frac{\partial}{\partial x_1}&\frac{\partial}{\partial x_2}&\frac{\partial}{\partial x_3}\end{bmatrix}\cdot\begin{bmatrix}0&\frac{\partial \xi_2}{\partial x_1}&0\\\frac{\partial \xi_2}{\partial x_1}&0&0\\0&0&0\end{bmatrix}=\mu\begin{bmatrix}0&\frac{\partial^2 \xi_2}{\partial x_1^2}&0\end{bmatrix} \tag{19}$$

This is qualitatively the same strain that the translating sphere of Figure 3 radiates at $\theta = \pi/2$. The difference is that rather than being an infinite plane wave, the amplitude of the strain field of the sphere is a function of the radial position of the point of observation.

Contrast this transverse shear strain with the longitudinal strain near a radially oscillating bubble. The individual, normal strains S_{rr}, $S_{\theta\theta}$ and $S_{\phi\phi}$ may be very large, but their sum $Tr\ \vec{\vec{S}}$ is extremely small because, as the bubble expands, the contraction in the radial strain is approximately canceled by the lateral dilatation. Thus, we have transverse and longitudinal shear waves. Both can have wave speeds that depend solely on the shear modulus of the medium (eqn [10]).

Shear strain is qualitatively the same in the two cases. For the transverse shear wave (Fig. 4), we show the cross section as a parallelogram, and its elements are off the diagonal (eqn [18]). For the longitudinal shear wave, we show the cross section of a strained element as a rectangle, and the elements of its strain tensor are on the diagonal (Fig. 5). Any second-order tensor can be diagonalized, of course. In fact, in a coordinate system rotated 45° from that shown in Figure 4, the strained element would appear as a rectangle. Strains of the elements are qualitatively the same. There is a fundamental difference, however. The transverse wave includes rigid rotation. The longitudinal wave involves translation of the element. All practical applications of elastography involve both transverse and longitudinal shear waves. Shear strains of sufficient amplitude can produce biological effects. It would be interesting to determine whether rigid rotation contributes independently to those effects as well.

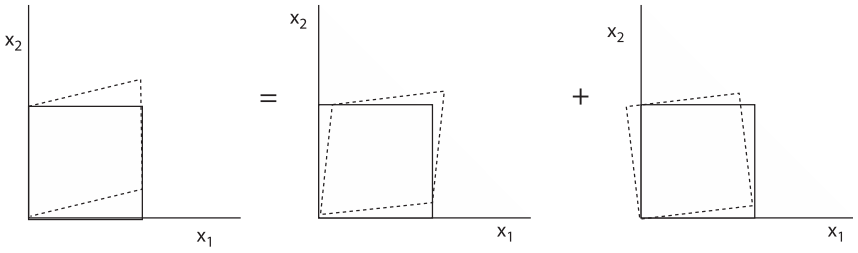

Fig. 4. An infinitesimal element in a medium, viewed in the (x_1, x_2) plane. A force is applied to the (x_2, x_3) interface in the x_2 direction. The force is balanced by the shear stiffness of the medium and inertial forces of the accelerating element's mass, creating a shear stress in the element. The result is a shear strain (a shape change) plus a rotation of the element (rightmost term in eqn [17]). The element does not change volume (trace = 0). As the force is removed, the elastic stress in the element returns it to its original shape and position. The motion of this element exerts a shear stress on its neighboring element to the right. The process repeats, resulting in a transverse shear wave moving in the x_1 direction.

$$\vec{\vec{S}} = A \begin{bmatrix} -1 & 0 & 0 \\ 0 & \frac{1}{2} & 0 \\ 0 & 0 & \frac{1}{2} \end{bmatrix}$$

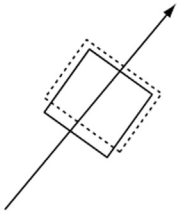

Fig. 5. Shear strain resulting from a radially oscillating bubble. The amplitude, A, is a strong function of the distance from the bubble. The shape of a cubical element morphs to that of a rectangular cuboid. When the radial component of the element contracts, the polar and azimuthal components expand, keeping the volume of the element approximately constant.

For greater relevance to elastography, we provide the strains for Oestreicher's translationally oscillating sphere along the axis of oscillation in Figure 6.

PART II: TISSUE MODELS

Elastography provides us with ever more accurate and detailed measurements of tissue shear moduli. Those data alone can be diagnostically useful simply through their correlation with clinical information. One may, however, presume that the information will become even more useful when we have a detailed understanding of the physical mechanisms that produce those stiffnesses.

It has become commonplace to use lumped element models from physical mechanics to represent the properties of tissues, which we know to be continua at the scale of shear wavelengths. Let us be clear about the limitations of this approach before proceeding to use it.

Equation (4) endows each arbitrary element of the propagating medium with two coincident properties, its density and its shear modulus. This might be represented by a parallel combination of a spring and a mass. It is activated by a difference in the force per unit area between the two ends and responds with a different displacement on one end than on the other.

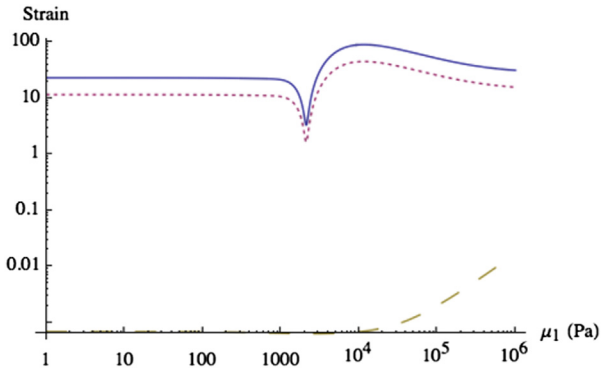

Fig. 6. Normalized, absolute value of the strains on the axis of a translationally oscillating sphere: radial longitudinal strain, S_{rr} (solid); transverse strain, $S_{\theta\theta}$, $S_{\phi\phi}$ (dotted); dilatational strain, $S_{rr} + 2S_{\theta\theta} = \Delta V/V$ (*dashed line*). All parameters are as used in Fig. 1 except $\theta = 0$.

At first glance, this appears to be a resonant system, and viewed as an isolated system, of course, it is. But we are modeling an arbitrarily small element of the medium. Changing the dimensions of the element changes the magnitudes of both components because we lump the values per unit volume into discrete elements. Lengthening the element decreases the stiffness and increases the mass. The resonance frequency of the element then depends on its dimensions. The element is resonant in the same sense that an organ pipe is resonant. It becomes a standing wave problem and is only indirectly related to the properties of the medium. There is no basis, therefore, to anticipate resonances in an infinite, homogeneous medium.

Furthermore, this first-order model does not include loss. In fact, the shear wave absorption coefficients of tissues are very large, and from the point of view of standing waves, most of the body's organs are effectively infinite in extent because of those losses. Elastography relies on the marked differences in stiffness between tumors and normal tissue. Considering the lossy nature of tissue and irregularities in tumor morphology, it seems unlikely that tissue "resonances" associated with the size and shape of elastic units will be useful clinically.

We can look at the resonance question in a slightly different way by keeping the elements representing the medium constant in size, but recognizing that each element is surrounded by similar elements. Consider the lower 1-D model in Figure 7. Apply a step force to the first element. The first mass accelerates to the right, compressing the spring, which simultaneously counters the motion of the mass and exerts increasing force on the adjacent element. Instead of a resonance oscillation, a wave propagates along the "infinite" line.

Stiffness mechanisms

At least two mechanisms give rise to the shear modulus, μ, in biological materials. To illustrate,

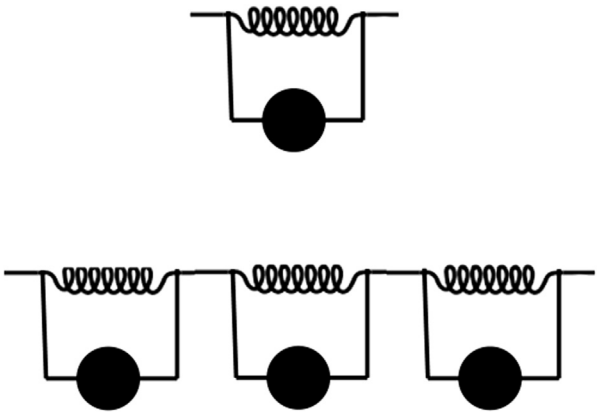

Fig. 7. Discrete element tissue models.

imagine measuring Young's modulus for a metal rod and compare that with a similar determination of the modulus for a rubber band. As the rod is stretched, energy is stored in the molecular bonds of the metal. Restoring force comes from the universal tendency of the material to seek a minimum in energy. Rubber is amorphous at a molecular level. Stretching reduces the number of states available, and entropy decreases. The primary restoring force in rubber comes from the universal tendency of entropy to increase. Although the two stiffnesses are fundamentally different, they both depend on the tendency of a system to minimize free energy, the ability to do work.

Many of the molecular constituents of tissue are similar to rubber in behavior. As examples, actin, which is a component of the cytoskeleton, and fibronectin, which contributes to the extracellular matrix, are globular when in solution, but become extended when functioning structurally. When subject to shear strain, these molecules behave as entropic springs. There are limits to this behavior, however. When the molecules approach a pure filamentous form, the intra-molecular bonds dominate the stiffness. So, there is a transition from maximizing entropy as the restoring factor to minimizing energy as the strain progresses. Little is known about the complexities of cellular architecture and its relationship to shear stiffness at the molecular level (Ingber 2003a, 2003b). The net result of the interaction of these energetic and entropic molecular springs is the macroscopic shear modulus, μ.

It turns out that we have a clue to the question of which mechanism dominates in specific cases from the temperature dependence of the stiffness. Molecular bonds tend to weaken as temperature increases. Entropic springs become stronger as temperature rises. Shear wave speed, therefore, should have a negative temperature coefficient in the first case and a positive coefficient when entropy dominates. In general, the elastography literature reports negative temperature coefficients of tissue wave speed. Kruse et al. (2000) report a negative temperature coefficient of approximately –2%/°C in excised bovine skeletal muscle.

Simple viscoelastic media

In the discussion up to this point, tissue has been treated as if it were composed of arbitrarily small elements each with a coincident stiffness and mass. The response of the tissue to force depends on the interaction of the stiffness and mass. Larger stiffnesses lead to smaller displacements and strains and higher speeds of propagation of perturbations through the medium. Larger densities lead to smaller displacements and slower propagation speeds. Nothing in this picture suggests that tissue absorbs acoustic energy. Wave speed should be dispersionless, and particle velocity should be in phase with the negative stress. If measurements indicate that this is not the case in tissue, it tells us that the model is either wrong or incomplete, and that indeed is what we find. In fact, shear waves used in elastography have far larger dispersions and absorption coefficients than the compressional waves used in medical ultrasound. The next step, then, must be to generalize the model to make it consistent with observations.

The simplest modification of the model, both analytically and conceptually, is to assume that tissue, like fluid, is viscous; that is, each element of the medium consists of coincident mass, stiffness and viscosity. (A word of caution before proceeding: The viscoelastic model has not been helpful in understanding the behavior of biological media in response to compressional stresses.)

The viscoelastic model says simply that stress is related to strain *and* time rate of change of the strain. In the general case,

$$\vec{\vec{T}} = \vec{\vec{c}}_1 \cdot \vec{\vec{S}} + \vec{\vec{c}}_2 \cdot \dot{\vec{\vec{S}}} \qquad (20)$$

where $\vec{\vec{c}}_1$ is the fourth-order elastic constant and $\vec{\vec{c}}_2$ is the corresponding viscosity, which we model as a dashpot in Figure 8. That would modify eqn (3) for applications of the viscoelastic case for any geometry. However, we will learn as much about models of the shear elasticity of tissues from the special case of a transverse plane wave (eqn [15]) as we would for a more general wave. For harmonic steady-state excitation, the time derivative becomes $j\omega$, and we can call the shear modulus $\mu = \mu_1 + j\omega\mu_2$, where μ_1 is the real shear modulus and μ_2 is the shear viscosity. The propagation constant becomes complex

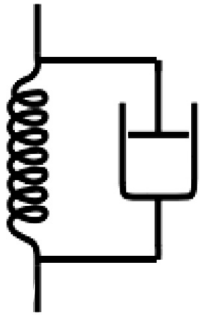

Fig. 8. The Kelvin-Voight parallel spring-dashpot model in mechanics has some of the properties of the coincident stiffness and viscosity assigned to the elements of an idealized viscoelastic medium. A parallel mass is implied.

$$k_s = \beta - j\alpha = \frac{\omega}{\sqrt{\frac{\mu_1 + j\omega\mu_2}{\rho}}} \tag{21}$$

and wave speed (eqn [10]) loses its simple meaning. Instead,

$$\vec{\xi}_2(x_1, t) = \vec{\xi}_2 e^{-\alpha x_1 + j(\omega t - \beta x_1)} \tag{22}$$

where

$$\alpha = \frac{\omega}{c_0}\left[\frac{1}{2}\frac{1}{1+\frac{\omega^2}{\omega_0^2}}\left(\sqrt{1+\frac{\omega^2}{\omega_0^2}} - 1\right)\right]^{1/2} \tag{23}$$

$$\beta = \frac{2\pi}{\lambda} = \frac{\omega}{c_0}\left[\frac{1}{2}\frac{1}{1+\frac{\omega^2}{\omega_0^2}}\left(\sqrt{1+\frac{\omega^2}{\omega_0^2}} + 1\right)\right]^{1/2} \tag{24}$$

$$c_0 = \sqrt{\frac{\mu_1}{\rho}} \tag{25}$$

and

$$\omega_0 = \frac{\mu_1}{\mu_2} \tag{26}$$

$\omega/\beta = c_{s\phi}$ is the shear velocity, the speed one must travel to stay at the same position or phase of the wave. Despite the fact that the viscoelastic model assumes a real, frequency-independent shear modulus for tissue, $c_{s\phi}$ is frequency dependent.

$$c_{s\phi} = c_0\left[\frac{1}{2}\frac{1}{1+\frac{\omega^2}{\omega_0^2}}\left(\sqrt{1+\frac{\omega^2}{\omega_0^2}} + 1\right)\right]^{-1/2} \tag{27}$$

At low frequencies,

$$c_{s\phi} \to c_0 \tag{28}$$

However, when $\omega >> \omega_0$,

$$c_{s\phi} \to c_0\sqrt{2\frac{\omega}{\omega_0}} \tag{29}$$

Thus, ω_0 is a characteristic or transition frequency that separates the low-frequency region in which the phase velocity is dominated by the stiffness of the tissue from the high-frequency region dominated by its viscosity.

With the introduction of a complex shear modulus, particle velocity is no longer in phase with stress, and the energy of the wave motion is gradually converted to heat as it propagates. The absorption coefficient α increases with the square of the frequency when

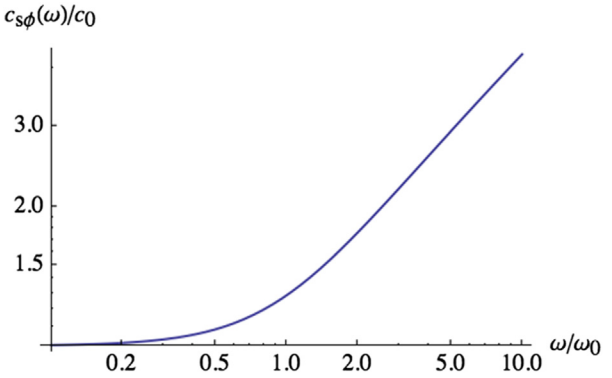

Fig. 9. Phase velocity predicted by the viscoelastic model (log-log plots).

$\omega << \omega_0$, and in the high-frequency limit $\omega >> \omega_0$, it is proportional to $\sqrt{\omega}$. The absorption per wavelength is

$$\alpha\lambda = 2\pi\left[\frac{\sqrt{1+\frac{\omega^2}{\omega_0^2}} - 1}{\sqrt{1+\frac{\omega^2}{\omega_0^2}} + 1}\right]^{1/2} \tag{30}$$

Although viscous absorption is small at low frequencies, it severely attenuates the wave at high frequencies, where $\alpha\lambda \to 2\pi$ (see Figs. 9–11).

Values of soft tissue shear moduli range upward from 1 kPa, viscosities in elastography applications range upward from 1 Pa s and densities are of the order of 1000 kg/m^3. Thus, values for c_0 range upward from 1 m/s, and typical frequencies of transition from stiffness dominance to viscosity dominance, ω_0, are of the order of 1000 rad/s or 100–200 Hz. Figure 10 illustrates that at the transition frequency ω_0, the absorption per wavelength is ~2; that is, the amplitude of the wave decreases by an order of magnitude in one wavelength (order of magnitude ~1 cm).

A fit of wave speed data to eqn (27) provides the complete determination of both of the elastic parameters,

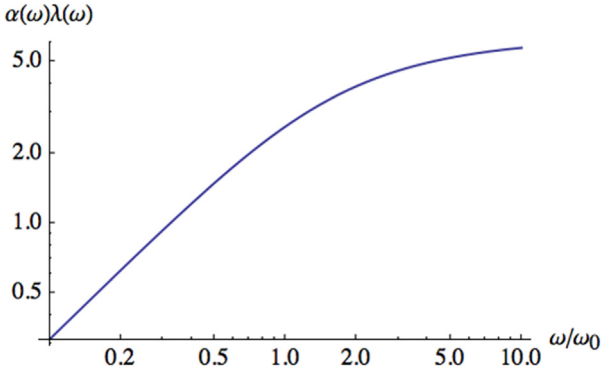

Fig. 10. Absorption per wavelength predicted by the viscoelastic model.

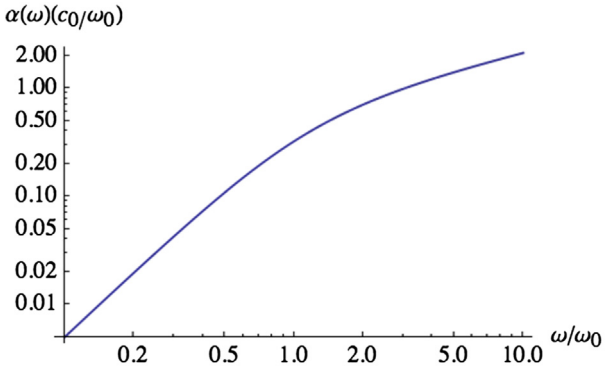

Fig. 11. Absorption predicted by the viscoelastic model.

as well as the absorption coefficient. Of course, the same is true for absorption data. Furthermore, if the viscoelastic model is appropriate, knowledge of the absorption coefficient and the wave speed at a single frequency is sufficient to compute the shear modulus and viscosity.

$$\mu_1 = \frac{\rho c_s^2}{\left(1-\frac{\alpha^2 c_s^2}{\omega^2}\right)\left(1+\frac{4\alpha^2 c_s^2}{\omega^2}\right)} \tag{31}$$

$$\mu_2 = \frac{\frac{2\rho\alpha}{c_s\omega^2}}{\frac{4\alpha^2}{c_s^2\omega^2}+\left(\frac{1}{c_s^2}-\frac{\alpha^2}{\omega^2}\right)^2} \tag{32}$$

In the real world, the shear wave speed can be measured with much higher precision than the shear wave absorption coefficient. (The reverse is true for irrotational waves used in conventional diagnostic ultrasound. In that case, the *dispersion* in the wave speed is so small that heroic efforts are required to measure it.) To determine the shear wave speed, all we need is the wavelength and the frequency. As long as there is a detectable signal, we need not be concerned with amplitude. This is fine for techniques such as sono-elastography that use single frequencies to excite the tissue. Interpreting the data is less obvious when the excitation is a pulse, as in radiation force elastography, or a step function, as in compression elastography.

Let us pause for a moment and consider how we might use shear waves to characterize tissues, increasing sophistication of the procedure with each step. (i) Simply determining wave speed provides us with valuable information. Normal liver, for example, has a wave speed in the range between 1.0 and 1.5 m/s. In cirrhotic liver, the speed exceeds 5 m/s. Many studies have reported a correlation of increasing wave speed with increasing degrees of fibrosis of the liver (Carstensen et al. 2008). (ii) Adding the absorption coefficient to the wave speed at a single frequency adds an additional number that can be correlated with the degree of health of tissue. In addition, those numbers can be given slightly more physical meaning by using them to compute the shear modulus and the shear viscosity of the tissue, using eqns (31) and (32). (iii) Measuring the wave speed (phase velocity) as a function of frequency and fitting those data to eqn (27) will also give both the shear stiffness and the shear viscosity of the tissue. Because wave speed can be measured with much greater precision *in vivo* than absorption, this method may be preferable to measurement of absorption for the determination of the viscosity.

Converting from acoustic observations to viscoelastic properties of tissue can change the way we think of the tissue. In reality, we are viewing the experimental measurements through the conceptual filter of the viscoelastic model. Whether this new view means more than the direct measurements depends a great deal on the validity of the model.

As formulated in the viscoelastic model, shear modulus and viscosity are simple constants, independent of time and frequency. If our observations are inconsistent with these assumptions, we are justified in concluding that the model is incomplete or in error.

Measurements of the shear properties of tissues are still limited. We do have enough information, however, to see that a simple viscoelastic model fails by orders of magnitude to describe the behaviors of tissue viscosities that have been actually observed. In contrast to the assumptions of the viscoelastic model, actual observations made under that assumption find viscosities at megahertz frequencies of the order of 0.01 Pa s, that is, only an order of magnitude greater than that of water (Frizzell et al. 1976; Madsen et al. 1983). However, below 1 kHz, the corresponding values are of the order of 10 Pa s (Oestreicher 1951). At both extremes of frequency, we could describe the behavior of tissue with a coincident shear modulus and shear viscosity ($\mu = \mu_1 + j\mu_2$) (Fig. 8), but the viscosities in the two local models of behavior would differ by around three orders of magnitude. The gap between these extremes of frequency has not been studied experimentally, but it is clear that a comprehensive model must allow for a shift between these two extremes of behavior.

Despite its limitations, the viscoelastic model has enduring status because it has become the default window through which we view our experimental data. We measure tissue properties as though they were in fact simple coincident stiffnesses, viscosities and masses, then qualify the results by describing the dependence of each parameter on variables such as frequency.

Relaxing media

This frequency dependence of the effective complex shear modulus can be understood as a form of acoustic relaxation. For our purposes, acoustic relaxation occurs when stress and energy are transmitted through the bulk medium to a time-sensitive internal system. There are many, possible, qualitatively different, relaxing processes. In addition to embedded or layered viscoelastic inclusions, we might conceivably consider contributions to shear stiffness from vibration and rotation of molecules, structural alterations of molecules, chemical processes and on and on—any internal system or combination of systems whose times for the response are comparable to the acoustic period.

When this model was used in studies of the propagation of conventional diagnostic ultrasound, it became clear that the bulk modulus of tissues could be attributed to water and similarly stiff tissue components. However, water and the other small molecules such as salts and amino acids contribute almost nothing to the propagation loss. Rather, the absorption is caused by the presence of macromolecules, not because of the increase in viscosity associated with their presence, but by pressure- or temperature-sensitive structural or chemical reactions in and among the molecules themselves. Furthermore, the structure of tissue plays only a secondary role in tissue absorption.

It would be helpful if we could use a thoroughly tested model of the shear properties of tissue to give realism to our discussion. Unfortunately, none exists. It still may be helpful if we use a purely speculative, but reasonable, model. So, let us say that the shear stiffness of the bulk tissue is determined by the large-scale structure of the tissue and that its viscosity is the actual viscosity of the fluids in and around the cells. Furthermore, let us say that the inner system is intercellular fluid passing through narrow spaces between cells, and therefore, the effective viscosity of this inner system is very large. This should not be equated to what has come to be called *poro-elasticity*. Poro-elasticity concerns the dynamics of squeezing fluid out of tissue; that is, the contents of the sample itself change during measurement (Berry et al. 2006). What we call the inner system is simply a tortuous path for the fluids in the sample, not a change in the fluid content of the sample. A realistic treatment of tissue with these properties would be extremely complex. However, the key difference between this problem and a simple viscoelastic medium is that the inner system is driven indirectly through the bulk medium. To illustrate the relaxation that occurs in such a system, we can think of a portion of the bulk medium as one spring-dashpot system, in series with (acting on) another parallel spring-dashpot combination, representing the internal system (Fig. 12). Although this model may be promising enough

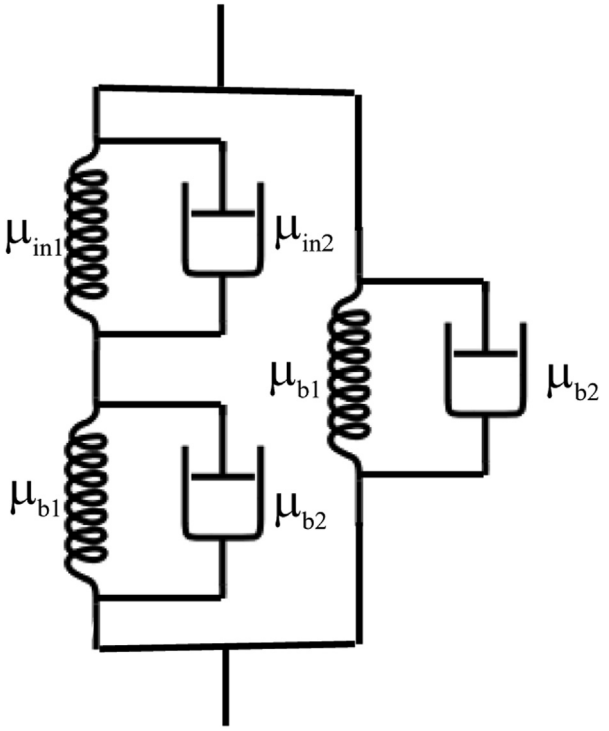

Fig. 12. Relaxation model. Stress is transferred through a portion of the bulk medium to an internal system.

to warrant serious testing, we use it here only to make the discussion less abstract.

In this simple example, we confine ourselves to only two shear moduli, $\mu_b = \mu_{b1} + j\omega\mu_{b2} = \mu_{b1}(1 + j(\omega/\omega_{0b}))$ for the bulk medium and $\mu_{in} = \mu_{in1} + j\omega\mu_{in2} = \mu_{in1}(1 + j(\omega/\omega_{0in}))$ for the internal system. Part of the medium is occupied by the internal system, and part of the bulk medium is in its path and serves as the coupler between the bulk and inner systems. Describing these systems in terms of their transition frequencies ω_{0b} and ω_{0in} instead of viscosities emphasizes the general nature of possible relaxation mechanisms.

Ignoring geometric details, the shear modulus of the series combination will have the form $\mu_b\mu_{in}/(\mu_b + \mu_{in})$. We must in some way account for the strength of the inner system, for example, the volume occupied by the inner spring-dashpot and the bulk system that couples to it. Let us just say that the space occupied by each of those components is the same and that the series combination occupies a volume fraction, f_v, of the medium. Then,

$$\mu = \mu_1 + j\omega\mu_2 = \mu_b(1 - f_v) + f_v\frac{\mu_b\mu_{in}}{\mu_b + \mu_{in}} \qquad (33)$$

Although no pretense is made that these assumptions will reproduce the properties of real tissues, this simple approach to the problem illustrates qualitatively the

frequency dependence that can be expected from the relaxation mechanism.

If tissue is as described in eqn (33) and we measure its effective shear stiffness and viscosity (*i.e.,* if we pretend that it is a simple viscoelastic medium), each quantity will be frequency dependent. As an example, assume a volume fraction for the inner system of 0.2, a stiffness of 1 kPa and a viscosity 20 Pa s; for the bulk system assume 10 kPa and 0.02 Pa s. This choice of parameters yields the general elastic behavior reported in the literature, in particular, the strong frequency dependence of the effective viscosity.

At low frequencies, the inner system contributes to the effective properties of the composite medium. At high frequencies, the large viscosity of the inner system essentially makes it rigid and it ceases to affect the composite system's elastic properties, leaving a simple viscoelastic system with properties of the bulk medium.

The corresponding shear wave speeds, c_s, and absorption coefficients, α, are given by

$$h = \frac{\omega}{\sqrt{\frac{\mu}{\rho}}} = \beta - j\alpha = \frac{\omega}{c_{s\phi}} - j\alpha \qquad (34)$$

where μ is defined by eqn (33).

Dispersion of the wave speed is small. It is characterized by plateaus below and above the relaxation frequency, corresponding respectively to the series combination of the moduli of the inner and bulk systems and the modulus of the bulk medium alone. Above the transition frequency for the bulk medium, the velocity increases with the square root of frequency (as it would for a simple viscoelastic medium). The absorption coefficient increases with the square of the frequency at low frequencies, plateaus above the relaxation frequency, then takes on the simple viscoelastic character of the bulk medium.

The example in Figures 13 and 14 and eqns (33) and (34) has been chosen to illustrate the relaxation concept in its simplest form. There is no reason in principle to believe that tissue has only one inner system. Probably the relaxation model should be written

$$\mu = \mu_1 + j\omega\mu_2 = A\mu_b + \sum_{i=1}^{N} B_i \frac{\mu_b \mu_{ini}}{\mu_b + \mu_{ini}} \qquad (35)$$

where A and B_i are appropriate weighting factors for the system under observation.

As suggested above, the frequency range covered by most elastography studies is too limited to rule out a simple viscoelastic model. Bot et al. (1997), however, have given us the complex shear modulus of a gelatin gel over the four decades from 100 Hz to 100 kHz. These data clearly cannot be described by a single, coincident shear stiffness and shear viscosity. The relaxation model of eqn (35) readily describes the data with four relaxing elements, one for each decade of the data. Note: Both real and imaginary parts of the shear modulus are simultaneously matched through this choice of strengths for the relaxing elements.

Although a simple viscoelastic model is clearly inadequate to explain the observed data for tissues and gels, Figures 13 and 15 illustrate that relaxation is a viable concept. Beyond its ability to represent empirical findings, the strongest support at present for the relaxation model is its physical and logical attractiveness. Most important, the relaxation model provides a framework for viewing empirical data. For it to have more value clinically than a purely phenomenological description of observations, it will be important to identify the specific relaxing elements of the tissues.

At first glance, it may seem that absorption and velocity should provide qualitatively different kinds of information. That is only partially true. The real stiffness, that is, the low-frequency limit of the shear modulus, is independent of absorption processes. However, in the models discussed thus far, the dispersion in the wave speed is related to the absorption. That conclusion is based on the Kramers-Kronig relations (Kronig 1926; Kramers 1927), which apply to all systems that are real and causal and whose response vanishes at infinite frequency. Rigorous application of those relationships is not realistic, and approximations have been formulated that relate local absorption to local dispersion (Carstensen and Schwan 1959b; O'Donnell et al. 1981). The approximations were developed for applications in which the magnitude of the dispersion is much smaller than the wave speed itself. It appears, however, that they give order-of-magnitude estimates even for shear waves at elastography frequencies. There is little question that potentially useful and possibly independent clinical information is contained in both the real and the imaginary components of the shear modulus. Whether that information is obtained through dispersion or absorption measurements is an engineering choice.

When we look at elastography data through the framework of the relaxation model, it adds character to our understanding of its implications for tissue even if we have only very general concepts of what the internal systems may be. (i) The low-frequency limit of the wave speed gives us *stiffness* for the composite material including the internal systems. (ii) The absorption coefficient (or, alternatively, dispersion in the wave speed) is determined almost entirely by the *viscous* properties of the *internal system*. We may hope that research will add greater meaning to the data when the internal systems are identified.

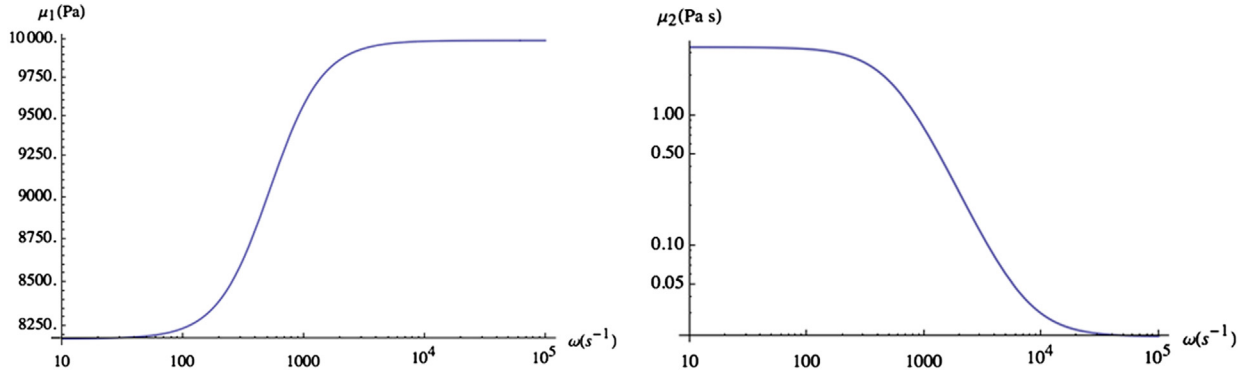

Fig. 13. Effective shear stiffness and viscosity predicted by eqn (33) with $p = 0.2$, $\mu_{b1} = 10$ kPa, $\mu_{b2} = 0.02$ Pa s and $\mu_{in1} = 1$ kPa, $\mu_{in2} = 20$ Pa s.

Hysteresis

Up to this point, we have considered only rate-sensitive loss systems, that is, systems in which the work delivered to the medium is proportional to the rate or velocity multiplied by time. These are probably the dominant mechanisms of absorption of shear waves in tissues and, perhaps, the only ones that need to be considered. There is a qualitatively different loss mechanism, however, that comes under the name of hysteresis, in which losses are directly proportional to displacements and independent of the rate (or the frequency) at which they take place. Hysteresis in the real world is very complex, and our discussion will be grossly oversimplified (Fig. 16).

Furthermore, it should be noted at this point that the entire discussion above describes material properties in the frequency domain. In the time domain, real materials do not have imaginary properties. However, as long as we limit our interest to sinusoidal, steady-state stresses and strains, the time domain response is just the real part of the complex response. Our interest is in material properties, not signal propagation, and that can be done most easily using the simplest forms of stress and strain. As a matter of interest, for rate-sensitive loss mechanisms, one can generalize to stresses with more complex time dependence using Fourier transforms. That may not be true for hysteresis even within definition. Please note, therefore, that the following is limited to sinusoidal, steady state stresses and strains.

Think of modeling clay as a purely hysteretic medium. Pretend that it is sheared in direct proportion to the stress applied. Once strained, it remains strained. There are no elastic forces to return it to its original state. In fact, the very concept of strain becomes arbitrary. If we approach the object again, in what sense is it more "strained" than it was when we first changed its shape? With problems like this, it is not surprising that specialists in the field find the classic model of hysteresis to be acausal (Crandall 1963, 1970; Muravskii 2004).

In the medical realm, you have only to see the indentations in your skin after removing tight-fitting clothing to be convinced that strain in tissue depends on its past history, as well as on the stress to which it is currently exposed. Pathology recognizes two forms of edema,

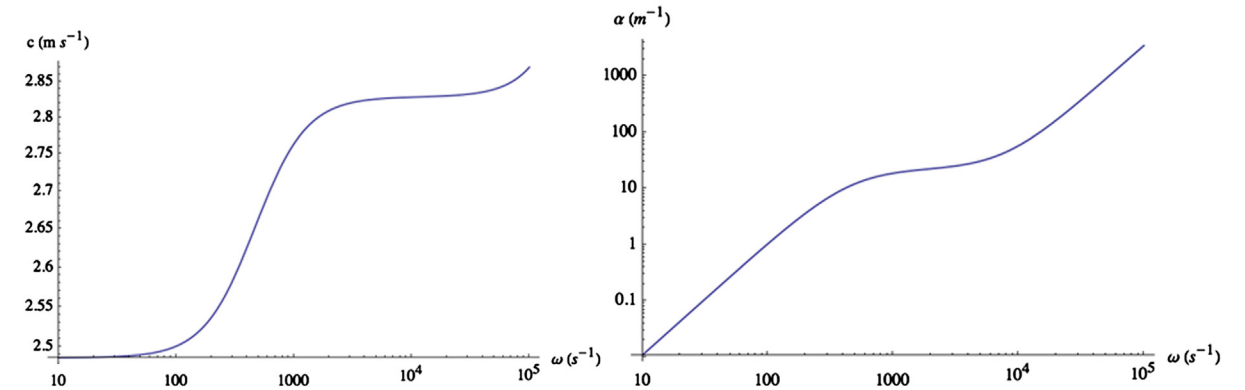

Fig. 14. Wave speed and absorption coefficient predicted by eqn (33) with $p = 0.2$, $\mu_{b1} = 10$ kPa, $\mu_{b2} = 0.02$ Pa s and $\mu_{in1} = 1$ kPa, $\mu_{in2} = 20$ Pa s.

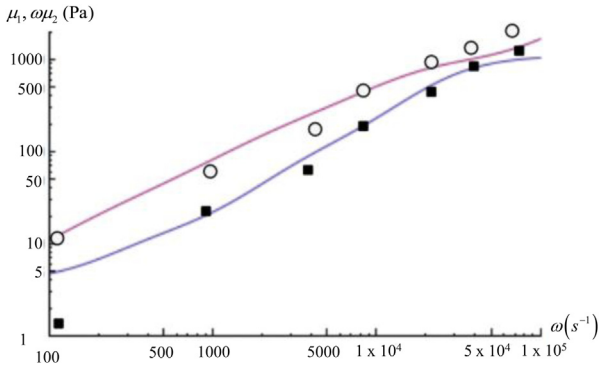

Fig. 15. Real (*solid squares*) and imaginary (*open circles*) parts of the complex shear stiffness of a 4% gelatin gel with a pH of 5.6 after 30 min of aging (Bot et al. 1997). The data were fitted by eqn (35) using four relaxing elements of comparable magnitudes and evenly spaced in the observed frequency range.

pitting and non-pitting. In the former, poking the region with a finger produces a long-lasting indentation. To extend the relaxation example that we introduced above (and to challenge your imagination), consider this possibility. In either form of edema, excess intra- and intercellular fluid accumulates in the tissue. In the extreme of pitting edema, perhaps the intercellular spaces become so constrained that they act more as valves than narrow pathways. Once strained, the tissue remains strained until forces from one source or another open the valves and return the fluid to its former location.

There is little doubt that the kind of response described here exists in many forms and that it is qualitatively different from rate-dependent loss mechanisms. The challenge is finding realistic physical models to describe it.

The prime characteristic that sets hysteresis apart from other mechanisms is a frequency-independent phase shift between a cause and an effect. There are a number of conclusions that follow from that assumption. These are all idealizations, but have implications about the usefulness of models of hysteresis.

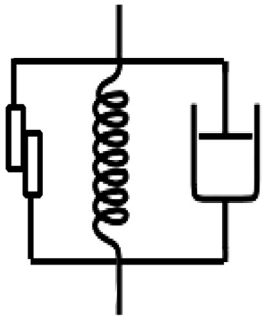

Fig. 16. Addition of hysteresis to the viscoelastic model. Our symbol for hysteresis should not suggest that it is equivalent to sliding friction, although there may be some properties in common.

First, in the absence of consensus, we need to define hysteresis carefully. There are two obvious possibilities: either we can say that hysteresis is a constant, frequency-independent phase lag of the strain relative to the applied stress (specifically, if the shear stress is $T = T_0\cos(\omega t) = \mathrm{Re}[T_0 e^{j\omega t}]$ the shear strain is $S = S_0\cos(\omega t - \phi) = \mathrm{Re}[S_0 e^{j(\omega t-\phi)}]$), or we can define hysteresis as constant loss per cycle. The second definition, in principle, is less restrictive.

Whereas eqn (2) is useful in the formulation of the wave equation, the definitions of hysteresis above clearly recognize stress as the independent variable. Instead of eqn (2), we need its inverse:

$$\vec{\vec{S}} = \vec{\vec{c}}^{-1} \cdot \vec{T} \tag{36}$$

If we restrict our interests to purely transverse stresses (off-diagonal elements of the stress tensor), we have simple scalar equations of the form

$$S = \frac{T_0 \cos(\omega t)}{2\mu} \tag{37}$$

and these equations serve our purpose in the investigation of the properties of hysteresis.

To include losses, we acknowledge that the shear modulus is complex and that the elements may be frequency dependent, $\mu = \mu_1 + j\mu_3$, where μ_3 will be the hysteresis modulus to distinguish it from viscosity, which we have called μ_2.

$$S = \mathrm{Re}\left[\frac{T_0 e^{j\omega t}}{2(\mu_1 + j\mu_3)}\right] = \frac{T_0}{2\sqrt{(\mu_1^2+\mu_3^2)}}\cos(\omega t - \phi) \tag{38}$$

where $\phi = \arctan(\mu_3/\mu_1)$.

Thus far, we have not characterized the frequency dependence of the shear modulus. The shear stiffness and the absorption resulting from hysteresis, in principle, are independent properties of material. It is difficult to imagine mechanisms that would make the frequency dependences of these independent parameters identical. Certainly, the simplest way to ensure a frequency-independent ϕ is to make both μ_3 and μ_1 independent of frequency. That, in turn, says that the ratio of amplitudes of the strain/stress is independent of frequency.

The energy per unit volume associated with a small change in strain is

$$dE = T\,dS = T\frac{dS}{dt}dt \tag{39}$$

$$dE = \frac{-\omega T_0^2 \cos(\omega t)\sin(\omega t-\phi)}{2\sqrt{(\mu_1^2+\mu_3^2)}}dt \tag{40}$$

And the energy lost per cycle is

$$\begin{aligned} E &= \int_0^{\frac{2\pi}{\omega}} \frac{-\omega T_0^2 \cos(\omega t)\sin(\omega t-\phi)}{2\sqrt{(\mu_1^2+\mu_3^2)}}dt \\ &= \frac{\pi T_0^2 \sin(\phi)}{2\sqrt{(\mu_1^2+\mu_3^2)}} = \frac{\pi T_0^2 \mu_3}{2(\mu_1^2+\mu_3^2)} \end{aligned} \tag{41}$$

or

$$E = 2\pi S_0^2 \mu_3 \tag{42}$$

where $S_0 = \frac{T_0}{2\sqrt{(\mu_1^2+\mu_3^2)}}$. Expressed in terms of strain, we have constant loss per cycle independent of frequency as long as the hysteresis modulus is a simple constant. The real part of the shear modulus can be arbitrary. Its value at any instant of time or at any frequency, as well as the magnitude of the stress, will affect S_0 and the phase between stress and strain. However, if we want, in addition, to have a frequency-independent phase lag, a common definition of hysteresis, both parameters will need to be constants independent of frequency.

With the understanding that the input is harmonic and steady state, we can compare wave propagation in a hysteretic medium with that in a viscoelastic medium. In this case, instead of eqn (36), eqn (2) becomes

$$T_{12} = (\mu_1 + j\mu_3)S_{12} \tag{43}$$

So the propagation constant

$$k = \beta - j\alpha = \frac{\omega}{c} - j\alpha = \frac{\omega}{\sqrt{\frac{\mu_1+j\mu_3}{\rho}}} \tag{44}$$

From this we obtain

$$\beta = \omega\sqrt{\frac{\rho}{\sqrt{\mu_1^2+\mu_3^2}}}\left[\frac{1}{2}\left(1+\frac{1}{\sqrt{1+\frac{\mu_3^2}{\mu_1^2}}}\right)\right]^{1/2} \tag{45}$$

The wave speed is independent of frequency

$$c = \sqrt{\frac{\sqrt{\mu_1^2+\mu_3^2}}{\rho}}\left[\frac{1}{2}\left(1+\frac{1}{\sqrt{1+\frac{\mu_3^2}{\mu_1^2}}}\right)\right]^{-1/2} \tag{46}$$

and the absorption coefficient is directly proportional to the first power of frequency, that is, a constant loss per cycle.

$$\alpha = \omega\sqrt{\frac{\rho}{\sqrt{\mu_1^2+\mu_3^2}}}\left[\frac{1}{2}\left(1-\frac{1}{\sqrt{1+\frac{\mu_3^2}{\mu_1^2}}}\right)\right]^{1/2} = \frac{\omega}{c}\sqrt{\frac{1-\frac{1}{\sqrt{1+\frac{\mu_3^2}{\mu_1^2}}}}{1+\frac{1}{\sqrt{1+\frac{\mu_3^2}{\mu_1^2}}}}} \tag{47}$$

For $\mu_1 >> \mu_3$,

$$c \to \sqrt{\frac{\mu_1}{\rho}} \tag{48}$$

and

$$\alpha \to \frac{\omega}{2c}\frac{\mu_3}{\mu_1} \tag{49}$$

For $\mu_1 << \mu_3$,

$$c \to \sqrt{\frac{2\mu_3}{\rho}} \tag{50}$$

$$\alpha \to \omega\sqrt{\frac{\rho}{2\mu_3}} = \frac{\omega}{c} \tag{51}$$

and

$$\alpha\lambda \to 2\pi \tag{52}$$

Mason (Mason and McSkimin 1947; Mason 1950) may have been the first to use this model in connection with ultrasound propagation. However, the basic idea as it applies to lumped mechanical elements goes back at least another decade, and in mechanical engineering, the quantity $\mu = \mu_1 + j\mu_3$ has gone under the names "linear structural damping," "hysteretic damper" and "ideal hysteretic damper." Makris (1997), in a relatively recent discussion, continues the use of this model. Although it grossly oversimplifies the full non-linear details of the stress-strain phenomenon, the Mason model captures two fundamental characteristics that set hysteresis apart from other loss mechanisms. First, loss per cycle is independent of the rate or frequency at which changes occur. This leads to an absorption that is proportional to the first power of frequency. Second, wave speed or phase velocity is dispersionless.

Mason's model only hints at the effects that hysteresis may have on shear wave propagation. Among other problems, it fails to deal with transients, particularly because Mason's model suggests that hysteresis is acausal. The imaginary part of the Fourier transform of its impulse response is even. Constant phase and the implications that property has for response independent of frequency are inconsistent with the basic Kramers-Kronig assumptions.

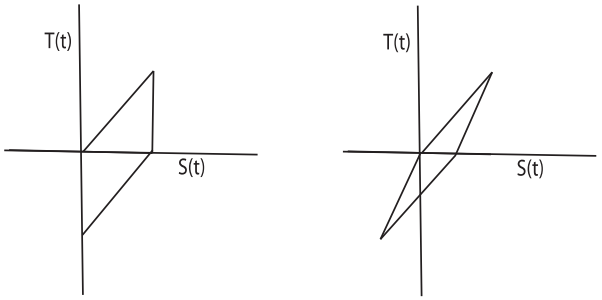

Fig. 17. Modeling clay as a hysteretic medium. On the left, $\mu_1 = 0$. When stress is removed, strain remains unchanged. Only by applying oppositely directed stress does strain return to its original state. On the right, $\mu_1 = \mu_3$. When stress is removed, the energy stored in the stiffness of the medium returns the strain partially to its original state.

In addition to being real and causal, Kramers-Kronig requires that the Cauchy integral converge at high frequency. Being independent of frequency makes that impossible. At best, the hysteresis concept, defined as constant loss per cycle, will be applicable only locally.

Returning to our modeling clay for a pure hysteretic medium, if you apply a shear stress and the clay is strained, it remains in that strained condition until you apply a shear stress in the opposite direction. So, instead of the smooth Lissajous figures predicted by eqn (43), we probably have non-linear hysteresis loops more like those in Figure 17. The precise nature of the hysteresis loop is of secondary interest. Fundamental differences between hysteresis and viscoelastic losses lie in the arbitrary nature of strain in the former. We can halt the hysteresis loop at any point and call that strain zero. Or we can say that the strain has an arbitrary value before we apply stress.

We clearly need a more sophisticated theoretical descriptor. More important, however, is the need for experimental studies, and those studies promise to be challenging in part because it may be difficult to separate the rate-dependent losses in tissues and phantoms from those that are not.

There is little doubt that a hysteresis-like phenomenon exists, and it would be surprising if it were not present in tissue. Because hysteresis differs physically at a fundamental level from viscoelastic processes and relaxation, finding clear evidence of hysteresis in tissues could have clinical value. Determining the role (if any) of hysteresis in tissues may require innovative experimental design.

CONCLUSIONS

The diagnostic value of ultrasound has come almost entirely from its ability to produce high-resolution images. Knowledge of the physical mechanisms responsible for the bulk elastic properties of tissues has been investigated for possible diagnostic value with little success. Perhaps this is so because there are only subtle differences in bulk stiffness among soft tissues and because the absorption mechanisms take place largely at a molecular level and involve complex and overlapping elements.

Elastography, in contrast, relies on the pronounced differences in shear stiffness among tissues and their abnormalities. Phenomenological descriptors of elastic properties are useful as placeholders. However, there is hope that models relating the physical characteristics of tissues to their observed shear parameters will be more informative. This review is merely a suggestion of the potential that a serious program of physical modeling might bring to clinical elastography.

Acknowledgments—The authors are indebted to Dr. Ted Christopher and Professors Sheryl Gracewski and Denise Hocking for many helpful comments.

REFERENCES

Amador C, Urban MW, Chen S, Greenleaf JF. Loss tangent and complex modulus estimated by acoustic radiation force creep and shear wave dispersion. Phys Med Biol 2012;57:1263–1282.

Bercoff J, Tanter M, Fink M. Supersonic shear imaging: A new technique for soft tissue elasticity mapping. IEEE Trans Ultrason Ferroelectr Freq Control 2004;51:396–409.

Berry GP, Bamber JC, Armstrong CG, Miller NR, Barbone PE. Towards an acoustic model-based poroelastic imaging method: I. Theoretical foundation. Ultrasound Med Biol 2006;32:547–567.

Bot A, Wientjes RHW, de Haas KH. The transition zone for gelatin gels as measured by high-frequency rheology. Imaging Sci J 1997;45:191–196.

Boursier J, Vergniol J, Sawadogo A, Dakka T, Michalak S, Gallois Y, Le Tallec V, Oberti F, Fouchard-Hubert I, Dib N, Rousselet MC, Konate A, Amrani N, de Ledinghen V, Cales P. The combination of a blood test and Fibroscan improves the non-invasive diagnosis of liver fibrosis. Liver Int 2009;29:1507–1515.

Carstensen EL, Parker KJ, Lerner RM. Elastography in the management of liver disease. Ultrasound Med Biol 2008;34:1535–1546.

Carstensen EL, Schwan HP. Absorption of sound arising from the presence of intact cells in blood. J Acoust Soc Am 1959a;31:185–189.

Carstensen EL, Schwan HP. Acoustic properties of hemoglobin solutions. J Acoust Soc Am 1959b;31:305–311.

Crandall SH. Dynamic response of systems with structural damping. In: Lees S, (ed). Air, space and instruments. New York: McGraw-Hill; 1963. p. 183–193.

Crandall SH. The role of damping in vibration theory. J Sound Vibration 1970;11:3–18.

Deffieux T, Gennisson JL, Muller M, Couade M, Bercoff J, Tanter M, Fink M. The supersonic shear imaging as a quantitative tool for imaging in vivo liver stiffness. In: Proceedings, 6th International Conference on the Ultrasonic Measurement and Imaging of Tissue Elasticity, Santa Fe, New Mexico, November 2–5, 2007:132.

Delingette H. Toward realistic soft-tissue modeling in medical simulation. Proc IEEE 1998;86:512–523.

Duck FA, Baker AC, Starritt HC. Ultrasound in medicine. Boca Raton, FL: CRC Press; 1998. p. 73.

Fatemi M, Greenleaf JF. Ultrasound-stimulated vibro-acoustic spectrography. Science 1998;280:82–85.

Frizzell LA, Carstensen EL, Dyro JF. Shear properties of mammalian tissues at low megahertz frequencies. J Acoust Soc Am 1976;60:1409–1411.

Fung YC. Biomechanics: Mechanical properties of living tissues. New York: Springer-Verlag; 1981.

Gao L, Parker KJ, Lerner RM, Levinson SF. Imaging of the elastic properties of tissue—A review. Ultrasound Med Biol 1996;22: 959–977.
Goss SA, Johnston RL, Dunn F. Comprehensive compilation of empirical ultrasonic properties of mammalian tissues. J Acoust Soc Am 1978;64:423–457.
Graff KF. Wave motion in elastic solids. Oxford: Clarendon Press; 1975.
Humphrey JD. Continuum biomechanics of soft biological tissues. Proc R Soc Lond A 2003;459:3–46.
Ingber DE. Tensegrity I: Cell structure and hierarchical systems biology. J Cell Sci 2003a;116:1157–1173.
Ingber DE. Tensegrity II: How structural networks influence cellular information processing networks. J Cell Sci 2003b;116: 1397–1408.
Kramers HA. La diffusion de la lumiere par les atomes. In: Atti del Congresso Internazionale dei Fisici, Como-Pavia-Roma, 11–20 Settembre 1927. Vol. 2. Bologna: N. Zanichelli, 1927:545–557.
Kronig RDL. On the theory of dispersion of x-rays. J Opt Soc Am 1926; 12:547–557.
Kruse SA, Smith JA, Lawrence AJ, Dresner MA, Manduca A, Greenleaf JF, Ehman RL. Tissue characterization using magnetic resonance elastography: Preliminary results. Phys Med Biol 2000; 45:1579–1590.
Lerner RM, Huang SR, Parker KJ. "Sonoelasticity" images derived from ultrasound signals in mechanically vibrated tissues. Ultrasound Med Biol 1990;16:231–239.
Lerner RM, Parker KJ, Holen J, Gramiak R, Waag RC. Sonoelasticity: Medical elasticity images derived from ultrasound signals in mechanically vibrated targets. Acoust Imaging 1988;16:317–327.
Madsen EL, Sathoff HJ, Zagzebski JA. Ultrasonic shear-wave properties of soft-tissues and tissuelike materials. J Acoust Soc Am 1983;74: 1346–1355.
Makris N. Causal hysteretic element. J Eng Mech 1997;123:1209–1214.
Mason WP. Piezoelectric crystals and their application in ultrasonics. New York: Van Nostrand; 1950. p. 482.
Mason WP, McSkimin HJ. Attenuation and scattering of high frequency sound waves in metals and glass. J Acoust Soc Am 1947;19: 464–473.
Mast TD, Hinkelman LM, Metlay LA, Orr MJ, Waag RC. Simulation of ultrasonic pulse propagation, distortion, and attenuation in the human chest wall. J Acoust Soc Am 1999;106:3665–3677.
McAleavey S, Collins E, Kelly J, Elegbe E, Menon M. Validation of SMURF estimation of shear modulus in hydrogels. Ultrason Imaging 2009;31:131–150.
Muravskii GB. On frequency independent damping. J Sound Vibration 2004;274:653–668.
Nachman AI, Smith JF, Waag RC. An equation for acoustic propagation in inhomogeneous-media with relaxation losses. J Acoust Soc Am 1990;88:1584–1595.
Nightingale K, Nightingale R, Palmeri M, Trahey G. Finite element analysis of radiation force induced tissue motion with experimental validation. In: Proceedings, 1999 IEEE International Ultrasonics Symposium, Caesar's Tahoe, Nevada, 17–20 October. Vol. 2. New York: IEEE, 1999:1319–1323.
Nightingale KR, Palmeri ML, Nightingale RW, Trahey GE. On the feasibility of remote palpation using acoustic radiation force. J Acoust Soc Am 2001;110:625–634.
O'Donnell M, Jaynes ET, Miller JG. Kramers-Kronig relationship between ultrasonic-attenuation and phase-velocity. J Acoust Soc Am 1981;69:696–701.
Oestreicher HL. Field and impedance of an oscillating sphere in a viscoelastic medium with an application to biophysics. J Acoust Soc Am 1951;23:704–714.
Ophir J, Cespedes I, Ponnekanti H, Yazdi Y, Li X. Elastography: A quantitative method for imaging the elasticity of biological tissues. Ultrason Imaging 1991;13:111–134.
Parker KJ, Doyley MM, Rubens DJ. Imaging the elastic properties of tissue: The 20 year perspective. Phys Med Biol 2011;56: R1–R29.
Pauly H, Schwan HP. Mechanism of absorption of ultrasound in liver tissue. J Acoust Soc Am 1971;50:692.
Salahura G, Tillett JC, Metlay LA, Waag RC. Large-scale propagation of ultrasound in a 3-D breast model based on high-resolution MRI Data. IEEE Trans Bio-Med Eng 2010;57:1273–1284.
Sandrin L, Fourquet B, Hasquenoph JM, Yon S, Fournier C, Mal F, Christidis C, Ziol M, Poulet B, Kazemi F, Beaugrand M, Palau R. Transient elastography: A new noninvasive method for assessment of hepatic fibrosis. Ultrasound Med Biol 2003;29: 1705–1713.
Sarvazyan AP, Rudenko OV, Swanson SD, Fowlkes JB, Emelianov SY. Shear wave elasticity imaging: A new ultrasonic technology of medical diagnostics. Ultrasound Med Biol 1998;24:1419–1435.
Sarvazyan AP, Skovoroda AR, Emelianov SY, Fowlkes JB, Pipe JG, Adler RS, Buxton RB, Carson PL. Biophysical bases of elasticity imaging. Acoust Imaging 1995;21:223–240.
Zhang M, Castaneda B, Wu Z, Nigwekar P, Joseph JV, Rubens DJ, Parker KJ. Congruence of imaging estimators and mechanical measurements of viscoelastic properties of soft tissues. Ultrasound Med Biol 2007;33:1617–1631.

APPENDIX

SYMBOLS

a radius of a sphere
c_0 low-frequency limit to the wave speed
c_s shear wave speed
$c_{s\phi}$ shear phase velocity, $c_{s\phi} = \omega/\beta$
c_d dilatational wave speed
$\overrightarrow{\overrightarrow{c}}$ fourth-order stiffness tensor: subscript 1 for real stiffness, subscript 2 for viscosity tensor
$\overrightarrow{e}_j$ unit spatial vector
f_v volume fraction
F_b force density
h propagation constant for shear waves; $h = \beta - j\alpha$
$j = \sqrt{-1}$
k propagation constant for compressional waves
λ wavelength
p pressure
r radial position
S strain
t time
T stress
Tr trace of a second-order tensor
x_j spatial coordinate
V volume (ΔV, change in volume)
α absorption coefficient
β real propagation constant
ϕ azimuth position angle
κ bulk modulus (κ_1, real bulk modulus; κ_2, bulk viscosity)
μ shear modulus (μ_1, real shear modulus; μ_2, shear viscosity; μ_3, hysteresis modulus)
θ polar position angle
ρ density
τ mean of dilatational stresses on an element of the medium
ξ particle displacement
ω angular frequency ω_0 transition frequency, μ_1/μ_2 for simple viscoelastic model
Ω rotation
∇ del operator: $\overrightarrow{e}_1\frac{\partial}{\partial x_1} + \overrightarrow{e}_2\frac{\partial}{\partial x_2} + \overrightarrow{e}_3\frac{\partial}{\partial x_3}$